Article title: Safety margin evaluations for transtympanic laser stimulation of the cochlea from the outer ear in Mongolian gerbils (*Meriones unguiculatus*)

List of author names: Aya Okamoto[1], Miku Uenaka[1], Yuki Ito[1], Tomohiro Miyasaka[2], Koji Toda[3], Shizuko Hiryu[1], Kohta I. Kobayasi[1*], Yuta Tamai[1,*]

Author affiliations:

[1]Neuroethology and Bioengineering, Graduate School of Life and Medical Sciences, Doshisha University, Kyotanabe, Kyoto, Japan

[2]Neuropathology, Graduate School of Life and Medical Sciences, Doshisha University, Kyotanabe, Kyoto, Japan

[3]Department of Psychology, Keio University, Tokyo, Japan

Corresponding author: Kohta I. Kobayasi and Yuta Tamai

(E-mail: kkobayas@mail.doshisha.ac.jp; ytamai@mail.doshisha.ac.jp)

Current address (Yuta Tamai): Neurobiology of Social Communication, Department of Otolaryngology-Head and Neck Surgery, Hearing Research Centre, University of Tübingen, Medical Center, Elfriede-Aulhorn-Strasse 5, 72076 Tübingen, Germany

Keywords

Auditory prosthesis, Infrared laser stimulation, Auditory perception, Head-fixed classical conditioning

Abstract

Infrared laser stimulation of the cochlea has been proposed as a possible alternative to conventional auditory prostheses. The safety margin of laser stimulation must be determined for the practical application of the laser to a prosthesis. This study assessed the effect of laser-induced damage to the cochlea on auditory perception. To examine the effects of laser-induced injury of the auditory system on the perception of auditory stimuli, we trained Mongolian gerbils (*Meriones unguiculatus*) using a head-fixed classical conditioning task. White noise of 80 dB sound pressure level (SPL) was presented as a conditioned stimulus for a reward (a drop of water), and licking behavior was recorded as a conditioned response. After training, an optic fiber was inserted into the ear canal. Each subject was exposed to continuous pulsed laser exposure of 1.6, 3.3, 6.6, 26.4, 52.8, or 105.6 W/cm^2 for 15 h. White noise of various intensities was presented without pairing it with water before and after laser exposure, to assess the decrease in auditory perception due to laser-induced injury. The licking rate did not change after laser exposure of 6.6 W/cm^2 or weaker but drastically decreased after 26.4 W/cm^2 or higher. These results suggest that the injury threshold in Mongolian gerbils for laser stimulation is between 6.6 and 26.4 W/cm^2; laser exposure over 6.6 W/cm^2 could be out of the safety margin. These findings will contribute to the appropriate delimitation of safe and effective laser

42 stimulation parameters in future research.

43

Introduction

Hearing impairment is a prevalent sensory disorder worldwide. Approximately 466 million people, 5% of the world's population, suffer from hearing deficits, resulting in severe communication difficulties and social isolation (World Health Organization, 2018, 2019, 2021). Hearing aids are among the most widely used therapeutic options to compensate for these problems. These devices improve speech comprehension and social interaction in hard-of-hearing individuals (Arlinger, 2003; Mulrow et al., 1990; Mulrow, Tuley, & Aguilar, 1992). However, these patients require an intact middle ear to ensure sufficient and proper hearing. Hard-of-hearing individuals with middle ear dysfunction must use an implantable auditory prosthesis (e.g., bone-anchored hearing devices, middle ear implants, or cochlear implants) that bypasses the function of the middle ear to stimulate the peripheral auditory system. One of the most significant drawbacks preventing the widespread use of these devices is surgical intervention, which increases the risk of complications post-surgery (Ahmed, Saqulain, Khan, & Kausar, 2021; Håkansson, Eeg-Olofsson, Reinfeldt, Stenfelt, & Granström, 2008; Yeung, Griffin, Newton, Kenna, & Licameli, 2018).

Infrared laser stimulation has been discussed as a possible alternative to conventional auditory devices (Littlefield & Richter, 2021). The advantage of laser

62 stimulation is that it can activate spatially focused cell populations in a non-contact
63 manner without the need to deliver any exogenous agent into tissues, such as a viral vector
64 (Fekete, Horváth, & Zátonyi, 2020). Early research by Izzo *et al.* (2006) suggested that
65 pulsed laser stimulation of the auditory nerves induced a cochlear response. Several later
66 studies that focused on the detailed relationship between the irradiation site of the cochlea
67 and laser-evoked neural response indicated that laser stimulation could elicit spatially
68 specific neural activities (Izzo, Suh, et al., 2007; Matic, Walsh, & Richter, 2011; Moreno
69 et al., 2011; Richter et al., 2011). That is, precisely manipulating the laser stimulation
70 system can improve the spectral resolution of cochlear implants. Our previous studies
71 leveraged the benefit of the contactless feature of laser stimulation to reduce the
72 invasiveness of surgical implantation of the auditory prosthesis. They revealed that
73 transtympanic laser stimulation from the outer ear could evoke a cochlear response,
74 bypassing the middle ear function (Tamai, Horinouchi, Hiryu, & Kobayasi, 2019; Uenaka,
75 Nagamura, Hiryu, Kobayasi, & Tamai, 2022). The auditory cortical activity elicited by
76 transtympanic laser stimulation depends on stimulus intensity (Tamai et al., 2020). These
77 results imply that a hearing prosthesis with infrared laser stimulation could be a
78 noninvasive alternative to the conventional implantable auditory prosthesis.

79 For the clinical application of transtympanic laser stimulation to auditory

prostheses, the safety margin of laser irradiation should be assessed. Because the laser-evoked neural response is probably related to the thermal elevation of the tissue (Albert et al., 2012; Shapiro, Homma, Villarreal, Richter, & Bezanilla, 2012; Wells et al., 2007), thermal build-up might be the main reason for laser-induced damage (Brown et al., 2020; Chernov, Chen, & Roe, 2014; Thompson, Wade, Pawsey, & Stoddart, 2013). Therefore, thermal damage to the peripheral auditory system can occur when a laser with high radiant energy is continuously presented. Some studies have investigated laser irradiation trauma in the cochlea (Izzo et al., 2006; Matic et al., 2013; Rajguru et al., 2010; Tamai et al., 2019). Goyal *et al.* (2012) compared the relationship between radiant energy in continuous laser exposure and the reduction of the laser-evoked electrophysiological response in the cochlea, reporting that the injury threshold for laser stimulation at 250 Hz was between 25 and 30 μJ/pulse. However, no study has described the influence of laser-induced thermal elevation on cochlear tissues or the effect of thermal physiological damage on auditory perception.

A comprehensive evaluation of laser irradiation trauma elucidates the effects of laser-induced damage on auditory perception. It provides a precise picture of the effect of laser stimulation on the auditory peripheral system. It assessed laser-induced damage characteristics of the peripheral auditory system by comparing electrophysiological,

98 histological, and behavioral alterations following continuous laser exposure. Here, we
99 performed (1) histological examination of spiral ganglions with hematoxylin and eosin
100 (HE) staining, (2) electrophysiological recording of the laser-evoked cochlear response
101 during laser irradiation, and (3) head-fixed classical conditioning with auditory stimulus
102 (see Figure 1 for details).
103
104 **Results**
105 Before the histological examination, the surface temperature of the cochlea was
106 recorded to investigate the thermal elevation following continuous laser irradiation
107 (Figure 2). The surface temperatures did not increase from 24 °C (i.e., room temperature)
108 using the 6.6 W/cm^2 laser irradiation or less; the laser 26.4 W/cm^2 or more increased the
109 surface temperatures immediately within 1 min into laser irradiation. The temperature
110 rise reached a plateau approximately 5 min after the laser onset (Figure 2A). Average
111 surface temperature at 10 min after the laser irradiation onset was described in Figure 2B
112 and showed that the increasing temperature induced by 26.4, 52.8, and 105.6 W/cm^2
113 lasers were 31.6, 36.6, and 44.7 °C, respectively. The ANOVA revealed that the effect of
114 radiant energy was statistically significant ($F(5,17)=21.26$, $P<0.001$, one-way ANOVA).
115 Figure 2C shows the lateral and medial surface temperatures induced by laser irradiation

116 at 105.6 W/cm^2 on the lateral side of the cochlea. The average temperatures of the lateral
117 and medial sides resulted in approximately 41.2 and 32.5 °C, respectively, and the
118 temperature difference between the left and the right sides was statistically significant
119 ($P<0.01$, paired t-test). The medial side temperature was approximately in line with that
120 of the lateral side irradiated by the laser at 26.4–52.8 W/cm^2.

121 Horizontal sections of the cochlea were subjected to HE staining to evaluate the
122 effect of laser exposure on the spiral ganglion neuron density (Figure 3A). Lower spiral
123 ganglion neuron density was found in the cochlea continuously irradiated by the laser of
124 105.6 W/cm^2 than in less than 6.6 W/cm^2 (Figure 3B). The middle turn of the cochlea
125 irradiated by the laser at 105.6 W/cm^2 is depicted in Figure 3C. A comparison of the
126 lateral and medial sides showed a remarkable decrease in the cell density on the lateral
127 side, mainly irradiated by the transtympanic laser, compared to the medial side. On the
128 lateral side of the cochlea, the spiral ganglion density difference between the left and right
129 ears significantly decreased ($r=-0.87$, $P<0.05$, Pearson's correlation analysis) as radiant
130 energy intensified, whereas on the medial side, it did not ($r=-0.45$, $P=0.23$, Pearson's
131 correlation analysis) (Figure 3D). The cell density decrement on the medial side after
132 laser exposure of 105.6 W/cm^2 approximately coincides with that on the lateral side
133 irradiated by the laser with 26.4–52.8 W/cm^2. Figure 3E shows the spiral ganglion neuron

134 density difference on the lateral side of the apical-middle and basal turn of the cochlea.
135 The apical-middle turn of the cell density in the left ear was significantly lower than that
136 in the right ear ($P<0.05$, one-sample t-test). In contrast, the basal turn of the cell density
137 was less affected than the apical-middle side ($P=0.19$, one-sample t-test) (Figure 3E).

138 Figure 4 shows the cochlear response after continuous laser exposure for 15 h. The
139 manifest damage in cochlear response was not observed by laser exposure up to 6.6
140 W/cm^2, while the cochlear response elicited by laser exposure of 105.6 W/cm^2 decreased
141 (Figure 4A). The time course of the relative response amplitude showed that continuous
142 laser exposure at 105.6 W/cm^2 caused a drastic decrease in the laser-evoked response
143 amplitude within ca. 65 min (Figure 4B). In comparison, laser irradiation of 6.6 W/cm^2
144 or less did not. Figure 4C shows the relationship between the laser irradiation time and
145 percentage of response amplitude. Laser irradiation over 26.4 W/cm^2 drastically increased
146 the average amplitude decrement, while laser stimulation with up to 26.4 W/cm^2 did not
147 (Figure 4D).

148 Figure 5A shows the licking behavior evoked by white noise (80 dB SPL) before
149 and after 1.6, 6.6, and 105.6 W/cm^2 laser exposure. The laser exposure at 1.6 and 6.6
150 W/cm^2 did not cause an observable behavioral response change, while an apparent
151 decrement of the licking rate was observed after 105.6 W/cm^2 laser exposure. The

behavioral changes after laser exposure are depicted in Figure 5B. Laser irradiation of the cochlea over 6.6 W/cm^2 drastically changed the behavioral level (Figure 5B). It caused the delta behavioral level (DBL) to reach out of the safety margin, which was calculated using three standard deviations of DBL in the control condition (Figure 5C).

159 **Discussion**

160 This study demonstrated that the laser stimulation with a higher average power
161 density triggered the thermal elevation of the cochlear surface (Figure 2). Because the
162 conventional mechanism of the laser-evoked cochlear response is the optothermal effect,
163 which causes an excessive temperature increase in the cells (Albert et al., 2012; Shapiro
164 et al., 2012; Wells et al., 2007), several studies indicated that laser-induced thermal
165 elevation and possible thermal-damage on the cochlea might constitute a significant
166 limitation in applying the laser to the auditory prosthesis (Goyal et al., 2012; Izzo, Walsh
167 Jr., et al., 2007; Matic et al., 2013; Rajguru et al., 2010; Thompson et al., 2013). Our study
168 demonstrated that cochlear surface temperature significantly increased as radiant energy
169 increased (Figure 2AB). The surface temperature continued to rise for approximately 5
170 min after laser onset, and then the elevated temperature reached a plateau (Figure 2A).
171 These results suggest that continuous laser irradiation (minute order) elevates cochlear
172 temperature compared with short-term irradiation. The continuous laser irradiation at
173 105.6 W/cm^2 caused an average surface temperature up to 44.7 °C, potentially causing
174 thermal tissue damage (Dewey, 1994). These results demonstrate that continuous laser
175 stimulation bears the risk of thermal damage to the cochlear tissues when a laser with
176 high radiant energy is used.

177 A comparison of the thermal elevation of the cochlear surface with histological
178 damage of spiral ganglion neurons revealed that the thermal distribution of the cochlear
179 surface affected the laser irradiation trauma of the spiral ganglion neurons. Our previous
180 study showed that transtympanic lasers mainly irradiated the middle turn of the lateral
181 side of the cochlea (Uenaka et al., 2022). This study implies that the highest peak of the
182 thermal distribution of the cochlear surface might be observed in the primary irradiated
183 area, and the temperature could decrease from the lateral to the medial side. It also showed
184 that the thermal elevation of the lateral side caused by laser irradiation of 105.6 W/cm^2
185 was significantly higher than that on the medial side. The 105.6 W/cm^2 laser-induced
186 temperature rise of the medial side reached 32.5 °C, which agreed with the lateral side
187 temperature caused by the laser at 26.4–52.8 W/cm^2 (Figure 2C). These results suggest
188 that approximately half of the radiant energy of laser irradiation reached the medial side
189 of the cochlea and agreed with the laser irradiation site in our previous study (Uenaka et
190 al., 2022). In addition, a more significant decrease in cell density was observed on the
191 lateral side of the apical-middle turn than on the basal turn (Figure 3E). These results
192 coincide with the radiant energy distribution (i.e., thermal distribution) of the cochlear
193 surface and suggest that the spatial injury profile of ganglion neurons depends on the
194 thermal distribution of the cochlear surface.

195 The electrophysiological cochlear response was recorded to evaluate the acute
196 damage threshold of continuous laser stimulation. This response is widely used as a
197 sensitive probe for physiological cochlear function (Prado-Guitierrez, Fewster, Heasman,
198 McKay, & Shepherd, 2006; Ramekers, Versnel, Strahl, Klis, & Grolman, 2015; van Eijl,
199 Buitenhuis, Stegeman, Klis, & Grolman, 2017). Previous studies, including ours (Izzo et
200 al., 2006; Rajguru et al., 2010; Tamai et al., 2019), have assessed laser-irradiation trauma
201 of the cochlea by recording the cochlear response induced by continuous laser stimulation.
202 These studies suggest that the laser safely evokes cochlear responses without causing
203 severe irradiation damage. However, Goyal *et al*. (2012) reported that continuous laser
204 irradiation with higher radiant energy induced thermal damage to the cochlear function.
205 This indicates that the injury threshold of laser exposure is between 25 and 30 μJ/pulse at
206 250 pulses/s (i.e., approximately 47.1 and 56.5 W/cm^2). Our results showed that the
207 cochlea kept responding to laser stimulation of 26.4 W/cm^2 or less, while the laser at 52.8
208 W/cm^2 or above remarkably decreased the cochlear response (Figure 4). This result
209 suggests that the electrophysiological damage threshold of the laser stimulation is
210 between 26.4 and 52.8 W/cm^2, and the injury threshold is in line with the previous study
211 by Goyal *et al*. (2012).

212 Measuring the impact of thermal-induced physiological deterioration in the cochlea

213 on auditory perception is crucial. Behavioral assessment of hearing loss generally
214 provides compelling evidence of auditory perceptual consequences following
215 compromised auditory processing. Therefore, evaluating auditory perception following
216 thermal injury in the cochlea is an essential step toward the clinical application of laser
217 stimulation to auditory prostheses. This study showed that the auditory-evoked licking
218 behavior did not change after laser exposure of 6.6 W/cm^2 or weaker, but drastically
219 decreased after 26.4 W/cm^2 or above. These results suggest that the thermal injury
220 threshold for transtympanic laser stimulation is between 6.6 and 26.4 W/cm^2. Therefore,
221 transtympanic laser stimulation over 6.6 W/cm^2 could be out of the safety margin.

222 A comparison of the behavioral and electrophysiological results revealed that the
223 thermal damage threshold for the auditory-evoked behavior alteration was slightly lower
224 than that for the laser-evoked cochlear response. Here, the laser irradiates the tympanic
225 membrane, auditory ossicles, and cochlear tissues from the outer ear to induce the
226 cochlear response (Uenaka et al., 2022); laser stimulation bears the risk of lesioning more
227 peripheral auditory function from the origin of the laser-evoked response. Our previous
228 study revealed that laser irradiation (λ=1871 nm) from the outer ear bypasses the
229 tympanic membrane and auditory ossicles because these tissues do not have higher
230 absorbance to the infrared laser (Uenaka et al., 2022). However, some studies investigated

231 the effect of the laser irradiation of the tympanic membrane and auditory ossicles in *vivo*
232 (Sorg et al., 2019) and in *vitro* (Pillong et al., 2020). This indicates that the laser irradiation
233 of 27.9 W/cm^2 or above at 532 nm could cause thermal damage. Although these results
234 are not directly comparable to our data because of the difference in wavelength-dependent
235 absorbance in the tympanic membrane and auditory ossicles, as some studies described
236 (Carr, Valdez, Bruns, & Bawendi, 2016; Goblet, Matin, Lenarz, & Paasche, 2021;
237 Heimann et al., 2021), thermal damage to the tympanic membrane and auditory ossicles
238 might be one reason why continuous laser exposure affects the auditory-evoked response
239 more than the laser-evoked response.

240 In addition to the tympanic membrane and auditory ossicles, hair cells in the
241 cochlea can be damaged by laser irradiation. The physiological mechanism of the laser-
242 evoked cochlear response is still debated whether the response is hair-cell-mediated
243 (Fekete et al., 2020). Hence, whether the laser-evoked response here characterized the
244 state of cochlear function is unclear, including that of hair cells. To reveal the
245 physiological mechanism of laser stimulation in the cochlea, some studies (Baumhoff,
246 Kallweit, & Kral, 2019; Schultz et al., 2012; Thompson et al., 2015) compared laser-
247 evoked auditory responses in normal hearing and chemically compromised cochlea and
248 reported that laser-evoked auditory responses were only observed in the normal hearing

249 cochlea. These studies suggest that the cochlear response elicited by laser stimulation is
250 mediated by hair cells.

251 In contrast, Richter *et al*. (2008) revealed that 30–40 dB chemical deafening of the
252 auditory threshold did not affect the threshold of the laser-evoked cochlear response. Tan
253 *et al*. (2018) demonstrated that laser stimulation could elicit auditory neural activity in
254 congenitally deaf mice in which the cochlea could not transmit synapses between the
255 inner hair cells and spiral ganglion neurons.

256 In addition, when animals have an impaired hearing threshold, auditory masking
257 does not affect laser-induced responses (Young, Tan, Xia, & Richter, 2015). These results
258 suggest that laser irradiation of the cochlea directly activates the auditory nerves,
259 bypassing hair cells. If the laser activates the cochlear nerves without needing hair cell
260 depolarization, the laser-evoked response does not characterize the state of the hair cells.
261 Therefore, our results show that the auditory-evoked response might be more vulnerable
262 to thermal injury than the laser-evoked response (Figures 4 and 5). The effect of thermal
263 damage to hair cells on laser-evoked cochlear responses must be considered in the future.

264 In summary, we assessed the laser-induced damage characteristics of the peripheral
265 auditory system through histological, electrophysiological, and behavioral tests.
266 Histological evaluation of the cochlea after continuous laser exposure revealed that the

laser-induced thermal distribution of the cochlear surface coincided with the spatial injury profile of spiral ganglion neurons. The measurement of auditory-evoked behavioral and laser-evoked electrophysiological responses indicate that cochlear response during the laser exposure of 26.4 W/cm^2 or weaker did not decrease. In contrast, auditory-induced behavioral response drastically decreased after 26.4 W/cm^2 or higher. This discrepancy in the injury threshold suggests that laser stimulation bears the risk of lesioning more peripheral auditory functions from the origin of the laser-evoked response. Evaluating perceptual consequences indicated that the thermal injury threshold for transtympanic laser stimulation in Mongolian gerbils is between 6.6 and 26.4 W/cm^2. Therefore, transtympanic laser under 6.6 W/cm^2 could be available without concern for acute injury. A comprehensive safety margin assessment is an essential step toward the practical application of transtympanic laser stimulation in auditory prostheses.

Acknowledgement

The authors would like to thank Hiroshi Riquimaroux for his support during the early stages of this work. We also thank Kazuki Tanaka, Mizuki Katayama, and Keito Hosokawa for technical support and Editage (www.editage.com) for English language editing. This research was financially supported by the Sasakawa Scientific Research

Grant No. 2022–6027 (A.O.), the Japan Society for the Promotion of Science (JSPS) KAKENHI Grants Nos. 22H02946 (T.M.), 21H03469 (K.I.K.), 21K21322 (Y.T.), the JSPS Overseas Research Fellowship (Y.T.), and Keio Academic Development Fund (K.T.).

Conflict of interests

The authors have no conflicts of interest to declare.

Materials and methods

Animals

All experimental procedures were performed according to the guidelines established by the Ethics Review Committee of Doshisha University. The experimental protocols were approved by the Animal Experimental Committee of Doshisha University. A total of 33 experimentally naive Mongolian gerbils (*Meriones unguiculatus*) aged 3–18 months were used here. All gerbils were bred and reared in a laboratory. Each animal was housed with 2–5 gerbils in a 20 (W) × 40 (L) × 17 cm (H) cage, with free access to food and water. The animal room had a 12-h light-dark schedule, a temperature of 22–23 °C, and relative humidity of approximately 50%.

Animal surgery

Mongolian gerbils were deeply anesthetized with ketamine (47 mg/kg i.m.) and

305 xylazine (9.3 mg/kg i.m.). Maintenance doses of ketamine (17.5 mg/kg) and xylazine (7.0
306 mg/kg) were injected every 30–50 min or if the animals showed signs of increasing
307 arousal (e.g., voluntary whisker movement). The body temperature of the gerbils was
308 maintained using heating pads placed beneath the animals. The left side of the bulla was
309 exposed by incision of the muscle and skin from the shoulder to the jaw, and a hole
310 (diameter: 1 mm) was made on the bulla. A silver electrode (Nilaco, Tokyo, Japan;
311 diameter: 0.13 mm; impedance < 20 kΩ) was inserted into the hole and hooked onto the
312 bony rim of the round window to record cochlear responses. The electrode was stabilized
313 with a bulla using acrylic glue and dental cement (Provinice; Shofu, Kyoto, Japan). The
314 left pinna was removed to provide a clear view of the tympanic membrane. A liquid of
315 acrylic glue and dental cement (Provinice; Shofu, Kyoto, Japan) was mounted into the
316 right ear for approximately 50 dB SPL attenuation of the sound pressure reaching the right
317 ear.

318 The parietal and temporal sides of the fur and the skin of the subject's head were
319 shaved. The temporal muscle was removed after applying a local anesthetic (xylocaine
320 gel; Aspen Japan, Tokyo, Japan). The skull was carefully cleaned with 0.3% sodium
321 hypochlorite solution and saline. A small hole was made in the dorsal skull 2 mm anterior
322 to the bregma and 1 mm lateral to the midline, and a reference electrode was inserted into
323 the hole. A V-shaped metal plate (F-911; Hilogik, Osaka, Japan) was attached to the skull
324 using acrylic dental resin (Super bond C&B; Sun Medical, Shiga, Japan) and dental
325 cement (Provinice; Shofu, Kyoto, Japan), allowing the subjects to be head-fixed during

326 the experiment. All subjects were singly housed during recovery for at least two days
327 before training began.

328 ***Auditory stimuli***

329 White noise (700–44,800 Hz) was used as an auditory stimulus, with a duration of
330 500 ms. The auditory stimulus was presented via a doom tweeter (FT28D; Fostex, Tokyo,
331 Japan) from 15 cm above the subject's head. The stimulus was generated using a digital-
332 to-analog converter (Octa-Capture; Roland, Shizuoka, Japan) with a sampling rate of 192
333 kHz. The signal was intensified using an amplifier (A-10; Pioneer, Tokyo, Japan). The
334 sound pressure level was calibrated to 20, 35, 50, 65, 80, and 95 dB SPL using a
335 microphone (Type 7016; Aco, Tokyo, Japan).

336 ***Apparatus and procedure in the behavioral experiment***

337 Behavioral experiments were conducted in a soundproof box 60 (W) × 60 (L) × 60
338 cm (H). Licking recordings in head-fixed animals were performed as previously described
339 (Guo et al., 2014; Kaneko et al., 2022; Toda et al., 2017; Yamamoto, Yamada, Yatagai,
340 Ujihara, & Toda, 2022). Each subject was positioned on a covered elevated platform
341 (custom-designed and 3D printed). A drinking spout was placed 1 mm in front of the
342 mouth of the animal, and the clamp and drinking spout positions were adjusted to detect
343 licking behavior easily. A touch sensor (DCTS-10; Sankei Kizai, Tokyo, Japan),

connected between the drinking spout and the metal sheet of the stage, recorded the timing of licks at 2000 samples/s. The recorded licking timing was stored on a computer via Arduino Uno (Arduino, Ivrea, Italy) controlled by Python 3.7 on Spyder 501. All behaviors were recorded using a video camera (HD-5000; Microsoft, Washington, USA).

After at least 2 days of recovery from surgery, the gerbils were water-restricted in their home cage. The training session typically comprised 400 trials daily. Head-fixed participants were allowed to voluntarily lick the spout at all times. A 3.2 μl drop of water (unconditioned stimulus: US) was delivered through the tube every 7–13 s after presenting an 85 dB SPL of white noise (conditioned stimulus: CS) controlled by MATLAB (MathWorks, Massachusetts, USA) and a microcontroller (Arduino Uno; Arduino, Ivrea, Italy) with a custom-made relay circuit.

After animals showed high licking rates following the auditory cue, catch trials were conducted to evaluate the subject's perception. The test session comprised rewarded and non-rewarded trials (i.e., catch trials). Catch trials were included to assess the subjects' perceptions without reward feedback. White noise of 20, 35, 50, 65, 80, or 95 dB SPL was presented in the catch trials. During a test session, 280 rewarded trials and 120 catch trials were conducted in a pseudo-random order. In the catch trials, each sound intensity was tested 20 times. The test session was performed pre- and post-laser exposure.

362 ***Recording and analysis of the behavioral data***

363 An averaged histogram of licking behavior was used to evaluate the time course of
364 behavioral responses. The histograms were calculated in a 100 ms bin size and
365 smoothened using a 300-ms moving average window. Peak licking rates, durations, peak
366 periods, and latencies were extracted from the time course of licking behavior to assess
367 the behavioral response. Peak licking rates and periods were defined as the licking rate
368 and time when the licking rate reached the maximum value within 4 s after stimulus onset,
369 respectively. The baseline licking rate was defined as the pre-stimulus licking rate
370 obtained for 1 s, and duration was quantified as the temporal length of licking behavior
371 >50% of the licking rate from the mean baseline licking rate to the peak licking rate.
372 Latency was determined by measuring the time between stimulus onset and the behavioral
373 response reaching the mean plus three standard deviations of the baseline licking rate.
374 The delta licking rate was defined as the difference between the mean baseline licking
375 rate and the post-stimulus licking rate to evaluate the response amplitude. The analysis
376 range of post-stimulus licking behavior was 0.2–1.2 s because the behavioral response
377 was mostly observed 0.2 s after stimulus onset (see Supplemental Figure 1 for details).
378 The behavioral level was calculated by standardizing the highest delta licking behavior
379 in the pre-exposure test. The delta behavioral level (DBL) between the pre- and post-

380 exposure test was defined as the summation of the difference in the behavioral level for
381 all sound pressure levels to evaluate the effect of continuous laser exposure on auditory
382 perception.

383 ***Laser exposure***

384 A repetitive pulsed infrared laser was used for laser exposure. The individual pulse
385 of the laser had a 100 μs rectangular shape in intensity. It was generated using a diode
386 laser stimulation system (BWF-OEM-1850; B&W TEK, Delaware, USA) with a
387 wavelength (λ=1871) comparable to those previously reported (Baumhoff et al., 2019;
388 Izzo et al., 2006; Izzo, Walsh Jr., et al., 2007). The voltage commands for the laser stimuli
389 were generated using a function generator (WF1974; NF, Kanagawa, Japan). The
390 repetition frequency of the pulsed laser was changed to 125, 250, 500, 2000, 4000, and
391 8000 Hz to adjust the amount of radiant energy reaching the cochlea to 1.6, 3.3, 6,6, 26.4,
392 52.8, and 105.6 W/cm^2, respectively. The radiant energy and beam width at the cochlea
393 (i.e., 2.2 mm from the fiber tip) were measured using a digital power meter (PM100D;
394 Thorlabs, Tokyo, Japan) with a thermal power sensor (S302C; Thorlabs, Tokyo, Japan)
395 and an InGaAs biased detector (DET10D/M; Thorlabs, Tokyo, Japan), respectively. Our
396 previous study measured the laser-beam profile (Uenaka et al., 2022).

397 An optic fiber (diameter: 100 μm; NA, 0.22) was inserted mediolaterally into the
398 left outer ear canal with the tip angled rostrally by 10° and dorsally by 5° using a
399 micromanipulator (MM-3; Narishige, Tokyo, Japan) in awake head-fixated subjects. The
400 optic fiber tip was set at c.a. 0.7 mm in front of the tympanic membrane to ensure that the
401 cochlea was irradiated transtympanically from the outer ear as described in our previous

402 reports (Tamai et al., 2019; Tamai et al., 2020; Uenaka et al., 2022).

403 Each subject's cochlea was continuously stimulated by laser irradiation from the
404 outer ear for 15 h. Continuous laser exposure was performed on the same covered elevated
405 platform in the soundproof box as in the behavioral experiment. The temperature in the
406 soundproof box was adjusted to approximately 26 ℃, and a small pee pad was placed
407 beneath the subject to prevent the subject's temperature from decreasing. After laser
408 exposure and behavioral experiments, the subjects were overdosed with an intraperitoneal
409 injection of pentobarbital (200 mg/kg). Laser-induced cochlear response was
410 continuously recorded throughout the study period. The cochleae were histologically
411 investigated to clarify the thermal damage caused by laser irradiation.

412 ***Recording and analysis of the cochlear response during laser exposure***

413 After the pre-exposure test, cochlear response was recorded in awake subjects
414 during continuous laser exposure. The cochlear response was amplified 1000 times using
415 a bio-amplifier (MEG-1200; Nihon Kohden, Tokyo, Japan) and stored on a computer via
416 an analog-to-digital converter (Octa-capture; Roland, Shizuoka, Japan) at a sampling rate
417 of 96,000 kHz.

418 The recorded signal was processed using a band-pass filter (100–10,000 Hz) and
419 separated at 10 ms intervals. The cochlear signal was averaged 1000 times every 10 s for
420 15 h, and the response amplitude of the averaged cochlear signal was evaluated using the
421 amplitude spectrum distribution. To obtain high-frequency resolution, 32,768 points of
422 zero paddings were performed on the head and end of the averaged signal. The amplitude
423 spectrum was extracted using fast Fourier transforms (FFT, 16,384 points with a Hanning
424 window); therefore, the frequency resolution was 5.9 Hz. The peak of the amplitude

425 spectrum at the stimulus repetition frequency was extracted as the response amplitude.
426 The mean response amplitude was calculated at 5 min intervals standardized by the first
427 5 min mean amplitude.

428 ***Preparation of histological evaluation***

429 Following the post-exposure test session, the laser-irradiated subjects were
430 euthanized by an overdose of pentobarbital (200 mg/kg i.p.). After postmortem perfusion
431 with phosphate buffered saline (PBS) and 4% paraformaldehyde in PBS, the animals were
432 decapitated and fixed in the same fixative for two days in a refrigerator at 4 ℃.
433 Subsequently, the tissues were stored in cooled PBS containing 0.02% sodium azide.

434 The paraformaldehyde-fixed tissues were decalcified by immersing in a mixture
435 solution of formic acid (0.28 g/ml), citric acid (0.1 g/ml), and sodium hydroxide (0.02
436 g/ml) for 7–10 days. The decalcifying solution was exchanged every 2–3 days. After the
437 decalcification, the samples were preserved in PBS with 0.02% sodium azide.

438 Decalcified head tissues were dehydrated using a gradually ascending
439 concentration of ethanol (70–100%) for 2 days followed by immersion in 100% xylene
440 and embedding into a paraffin block. Horizontally, paraffin-embedded sections with the
441 thickness of 6 μm was processed using a microtome (HM 430; Thermo, Tokyo, Japan).

442 Cochlear sections between 7 and 8 mm ventral to the sagittal midline from each

443 subject were examined. Sections were deparaffinized by immersion in 100% xylene.
444 After the deparaffinization, sections were hydrated with 100% ethanol and distilled water.
445 Sections were stained with Mayer's hematoxylin solution and rinsed with distilled water.
446 After differentiation with 70% ethanol containing 0.1% HCL, the sections were stained
447 with Putt's eosin solution. HE-stained sections were re-immersed in 100% ethanol and
448 cleared in xylene. All stained sections were mounted in mounting medium (HSR solution;
449 Sysmex, Hyogo, Japan). Specimens were photographed using a digital camera (BX53;
450 Olympus, Tokyo, Japan) under a light microscope (EX-F1; Casio, Tokyo, Japan).
451 Histological analysis was performed using ImageJ software (Abràmoff, Magalhães, &
452 Ram, 2004; Schneider, Rasband, & Eliceiri, 2012).

453 ***Behavioral data analysis for a safety margin evaluation***

454 Each subject was placed on a covered elevated platform for 15 h in a temperature-
455 controlled soundproof box, similar to the laser exposure experiment without presenting
456 laser irradiation. We compared the performance of the classical conditioning task before
457 and after placement on the covered elevated platform. The mean and standard deviation
458 of the control condition were measured to determine the safety margin of continuous laser
459 irradiation. The safety margin was defined as the mean ± three standard deviations of
460 the DBL in the control condition (n=9).

461 ***Correlation between physiological damage in the cochlea and behavioral alternation***

462 To determine whether these histological and functional deficits in the cochlea were
463 associated with behavioral alterations, we correlated the change in spiral ganglion neuron
464 density and amplitude of the cochlear response with the behavioral response. Further
465 details are provided in Supplemental Figure 2.

466 ***Recording thermal elevation of the cochlear surface***

467 Eleven gerbils were euthanized (pentobarbital; 200 mg/kg) and decapitated for
468 cochlear surface thermal measurements. Both sides of the cochlea were extracted from
469 the skulls under a stereomicroscope. The cochlea was placed in a Petri dish and stabilized
470 with dental wax. The laser fiber tip was directed vertically to the surface of the cochlea
471 and was set to 2.2 mm from the cochlear surface. Continuous laser irradiation with 1.6,
472 3.3, 6.6, 26.4, 52.8, and 105.6 W/cm^2 was performed for 1 h, and the surface temperature
473 elevations were measured using a thermal camera (FLIR C3-X; Teledyne FLIR LLC,
474 Oregon, USA), which was positioned at 21 cm from the cochlear surface with vertically
475 45° angle.

476 To acquire the thermal elevation on the lateral and medial sides of the cochlear
477 surface, a thermocouple (MSM-3905; Biomedica, Osaka, Japan) was used. The tip of the
478 thermocouple sensor was in contact with the second turn of the cochlear surface on one

side for 1 h. After recording the temperature on one side, the specimen was left for at least 15 min to cool down to room temperature (~24 °C), and then the temperature on another side was measured.

Flow of the behavioral, electrophysiological, and histological procedure

Surgery, behavior training, pre-exposure test, laser exposure for 15 h, post-exposure test, and histological evaluation were performed in this order. The recovery period was performed after surgery before and after laser exposure. Further details are provided in Figure 1.

References

Abràmoff, M. D., Magalhães, P. J., & Ram, S. J. (2004). Image processing with ImageJ. *Biophotonics int., 11*(7), 36-42.

Ahmed, J., Saqulain, G., Khan, M. I. J., & Kausar, M. (2021). Complications of cochlear implant surgery: A public implant centre experience. *Pak. J. Med. Sci., 37*(5), 1519-1523. doi:10.12669/pjms.37.5.3960

Albert, E. S., Bec, J. M., Desmadryl, G., Chekroud, K., Travo, C., Gaboyard, S., . . . Chabbert, C. (2012). TRPV4 channels mediate the infrared laser-evoked response in sensory neurons. *J. Neurophysiol., 107*(12), 3227-3234. doi:10.1152/jn.00424.2011

Arlinger, S. (2003). Negative consequences of uncorrected hearing loss-a review. *Int. J. Audiol., 42 Suppl 2*, 2s17-20.

Baumhoff, P., Kallweit, N., & Kral, A. (2019). Intracochlear near infrared stimulation: Feasibility of optoacoustic stimulation in vivo. *Hear. Res., 371*, 40-52. doi:10.1016/j.heares.2018.11.003

Brown, W. G. A., Needham, K., Begeng, J. M., Thompson, A. C., Nayagam, B. A., Kameneva, T., & Stoddart, P. R. (2020). Thermal damage threshold of neurons during infrared stimulation. *Biomed. Opt. Express, 11*(4), 2224-2234. doi:10.1364/boe.383165

Carr, J. A., Valdez, T. A., Bruns, O. T., & Bawendi, M. G. (2016). Using the shortwave infrared to image middle ear pathologies. *Proc. Natl. Acad. Sci. U S A, 113*(36), 9989-9994. doi:10.1073/pnas.1610529113

Chernov, M. M., Chen, G., & Roe, A. W. (2014). Histological assessment of thermal damage in the brain following infrared neural stimulation. *Brain. Stimul., 7*(3), 476-482. doi:10.1016/j.brs.2014.01.006

Dewey, W. C. (1994). Arrhenius relationships from the molecule and cell to the clinic. *Int. J. Hyperthermia, 10*(4), 457-483. doi:10.3109/02656739409009351

Fekete, Z., Horváth, Á. C., & Zátonyi, A. (2020). Infrared neuromodulation: A neuroengineering perspective. *J. Neural. Eng., 17*(5), 051003. doi:10.1088/1741-2552/abb3b2

Goblet, M., Matin, F., Lenarz, T., & Paasche, G. (2021). Optical absorbance of the tympanic membrane in rat and human samples. *PLoS One, 16*(7), e0254902. doi:10.1371/journal.pone.0254902

Goyal, V., Rajguru, S., Matic, A. I., Stock, S. R., & Richter, C. P. (2012). Acute damage threshold for infrared neural stimulation of the cochlea: functional and

histological evaluation. *Anat. Rec. (Hoboken), 295*(11), 1987-1999. doi:10.1002/ar.22583

Guo, Z. V., Hires, S. A., Li, N., O'Connor, D. H., Komiyama, T., Ophir, E., . . . Svoboda, K. (2014). Procedures for behavioral experiments in head-fixed mice. *PLoS One, 9*(2), e88678. doi:10.1371/journal.pone.0088678

Håkansson, B., Eeg-Olofsson, M., Reinfeldt, S., Stenfelt, S., & Granström, G. (2008). Percutaneous versus transcutaneous bone conduction implant system: A feasibility study on a cadaver head. *Otol. Neurotol., 29*(8), 1132-1139. doi:10.1097/MAO.0b013e31816fdc90

Heimann, L., Carlein, C., Sorg, K., Diller, R., Langenbucher, A., Schick, B., & Wenzel, G. I. (2021). Wavelength-specific optoacoustic-induced vibrations of the guinea pig tympanic membrane. *J. Biomed. Opt., 26*(3), 038001. doi:10.1117/1.Jbo.26.3.038001

Izzo, A. D., Richter, C. P., Jansen, E. D., & Walsh Jr., J. T. (2006). Laser stimulation of the auditory nerve. *Lasers Surg. Med., 38*(8), 745-753. doi:10.1002/lsm.20358

Izzo, A. D., Suh, E., Pathria, J., Walsh, J. T., Whitlon, D. S., & Richter, C. P. (2007). Selectivity of neural stimulation in the auditory system: A comparison of optic and electric stimuli. *J. Biomed. Opt., 12*(2), 021008. doi:10.1117/1.2714296

Izzo, A. D., Walsh Jr., J. T., Jansen, E. D., Bendett, M., Webb, J., Ralph, H., & Richter, C. P. (2007). Optical parameter variability in laser nerve stimulation: A study of pulse duration, repetition rate, and wavelength. *IEEE Trans. Biomed. Eng., 54*(6), 1108-1114. doi:10.1109/TBME.2007.892925

Kaneko, S., Niki, Y., Yamada, K., Nasukawa, D., Ujihara, Y., & Toda, K. (2022). Systemic injection of nicotinic acetylcholine receptor antagonist mecamylamine affects licking, eyelid size, and locomotor and autonomic activities but not temporal prediction in male mice. *Mol. Brain., 15*(1), 77. doi:10.1186/s13041-022-00959-y

Littlefield, P. D., & Richter, C. P. (2021). Near-infrared stimulation of the auditory nerve: A decade of progress toward an optical cochlear implant. *Laryngoscope Investig. Otolaryngol., 6*(2), 310-319. doi:10.1002/lio2.541

Matic, A. I., Robinson, A. M., Young, H. K., Badofsky, B., Rajguru, S. M., Stock, S., & Richter, C. P. (2013). Behavioral and electrophysiological responses evoked by chronic infrared neural stimulation of the cochlea. *PLoS One, 8*(3), e58189. doi:10.1371/journal.pone.0058189

Matic, A. I., Walsh, J. T., Jr., & Richter, C. P. (2011). Spatial extent of cochlear infrared

neural stimulation determined by tone-on-light masking. *J. Biomed. Opt., 16*(11), 118002. doi:10.1117/1.3655590

Moreno, L. E., Rajguru, S. M., Matic, A. I., Yerram, N., Robinson, A. M., Hwang, M., . . . Richter, C. P. (2011). Infrared neural stimulation: Beam path in the guinea pig cochlea. *Hear. Res., 282*(1-2), 289-302. doi:10.1016/j.heares.2011.06.006

Mulrow, C. D., Aguilar, C., Endicott, J. E., Tuley, M. R., Velez, R., Charlip, W. S., . . . DeNino, L. A. (1990). Quality-of-life changes and hearing impairment. A randomized trial. *Ann. Intern. Med., 113*(3), 188-194. doi:10.7326/0003-4819-113-3-188

Mulrow, C. D., Tuley, M. R., & Aguilar, C. (1992). Sustained benefits of hearing aids. *J. Speech Hear. Res., 35*(6), 1402-1405. doi:10.1044/jshr.3506.1402

Pillong, L., Stahn, P., Hinsberger, M., Sorg, K., Schick, B., & Wenzel, G. I. (2020). Cytotoxicity studies of an optoacoustic stimulation strategy for the development of laser-based hearing aids. *J. Biomed. Opt., 25*(6), 068002. doi:10.1117/1.Jbo.25.6.068002

Prado-Guitierrez, P., Fewster, L. M., Heasman, J. M., McKay, C. M., & Shepherd, R. K. (2006). Effect of interphase gap and pulse duration on electrically evoked potentials is correlated with auditory nerve survival. *Hear. Res., 215*(1-2), 47-55. doi:10.1016/j.heares.2006.03.006

Rajguru, S. M., Matic, A. I., Robinson, A. M., Fishman, A. J., Moreno, L. E., Bradley, A., . . . Richter, C. P. (2010). Optical cochlear implants: evaluation of surgical approach and laser parameters in cats. *Hear. Res., 269*(1-2), 102-111. doi:10.1016/j.heares.2010.06.021

Ramekers, D., Versnel, H., Strahl, S. B., Klis, S. F., & Grolman, W. (2015). Recovery characteristics of the electrically stimulated auditory nerve in deafened guinea pigs: Relation to neuronal status. *Hear. Res., 321*, 12-24. doi:10.1016/j.heares.2015.01.001

Richter, C. P., Bayon, R., Izzo, A. D., Otting, M., Suh, E., Goyal, S., . . . Walsh Jr., J. T. (2008). Optical stimulation of auditory neurons: Effects of acute and chronic deafening. *Hear. Res., 242*(1-2), 42-51. doi:10.1016/j.heares.2008.01.011

Richter, C. P., Rajguru, S. M., Matic, A. I., Moreno, E. L., Fishman, A. J., Robinson, A. M., . . . Walsh, J. T. (2011). Spread of cochlear excitation during stimulation with pulsed infrared radiation: Inferior colliculus measurements. *J. Neural. Eng., 8*(5), 056006. doi:10.1088/1741-2560/8/5/056006

Schneider, C. A., Rasband, W. S., & Eliceiri, K. W. (2012). NIH Image to ImageJ: 25

years of image analysis. *Nat. Methods., 9*(7), 671-675. doi:10.1038/nmeth.2089

Schultz, M., Baumhoff, P., Maier, H., Teudt, I. U., Kruger, A., Lenarz, T., & Kral, A. (2012). Nanosecond laser pulse stimulation of the inner ear-a wavelength study. *Biomed. Opt. Express, 3*(12), 3332-3345. doi:10.1364/boe.3.003332

Shapiro, M. G., Homma, K., Villarreal, S., Richter, C. P., & Bezanilla, F. (2012). Infrared light excites cells by changing their electrical capacitance. *Nat. Commun., 3*, 736. doi:10.1038/ncomms1742

Sorg, K., Stahn, P., Pillong, L., Hinsberger, M. P., Heimann, L., Foth, H. J., . . . Wenzel, G. I. (2019). First biocompatibility margins for optical stimulation at the eardrum via 532-nm laser pulses in a mouse model. *J. Biomed. Opt., 24*(8), 085003. doi:10.1117/1.Jbo.24.8.085003

Tamai, Y., Horinouchi, K., Hiryu, S., & Kobayasi, K. I. (2019). Infrared laser stimulation of cochlear nerve through a tympanic membrane. *Conf. Proc. IEEE Life Sci. Tech. 2019, 1*(1), 54-57. doi:10.1109/LifeTech.2019.8884023

Tamai, Y., Ito, Y., Furuyama, T., Horinouchi, K., Murashima, N., Michimoto, I., . . . Kobayasi, K. I. (2020). Auditory cortical activity elicited by infrared laser irradiation from the outer ear in Mongolian gerbils. *PLoS One, 15*(10), e0240227. doi:10.1371/journal.pone.0240227

Tan, X., Jahan, I., Xu, Y., Stock, S., Kwan, C. C., Soriano, C., . . . Richter, C. P. (2018). Auditory neural activity in congenitally deaf mice induced by infrared neural stimulation. *Sci. Rep., 8*(1), 388. doi:10.1038/s41598-017-18814-9

Thompson, A. C., Fallon, J. B., Wise, A. K., Wade, S. A., Shepherd, R. K., & Stoddart, P. R. (2015). Infrared neural stimulation fails to evoke neural activity in the deaf guinea pig cochlea. *Hear. Res., 324*, 46-53. doi:10.1016/j.heares.2015.03.005

Thompson, A. C., Wade, S. A., Pawsey, N. C., & Stoddart, P. R. (2013). Infrared neural stimulation: Influence of stimulation site spacing and repetition rates on heating. *IEEE Trans. Biomed. Eng., 60*(12), 3534-3541. doi:10.1109/TBME.2013.2272796

Toda, K., Lusk, N. A., Watson, G. D. R., Kim, N., Lu, D., Li, H. E., . . . Yin, H. H. (2017). Nigrotectal stimulation stops interval timing in mice. *Curr. Biol., 27*(24), 3763-3770.e3763. doi:10.1016/j.cub.2017.11.003

Uenaka, M., Nagamura, H., Hiryu, S., Kobayasi, K. I., & Tamai, Y. (2022). Feasibility evaluation of transtympanic laser stimulation of the cochlea from the outer ear. *J. Acoust. Soc. Am., 152*(3), 1850-1855. doi:10.1121/10.0014241

van Eijl, R. H., Buitenhuis, P. J., Stegeman, I., Klis, S. F., & Grolman, W. (2017).

Systematic review of compound action potentials as predictors for cochlear implant performance. *Laryngoscope, 127*(2), 476-487. doi:10.1002/lary.26154

Wells, J., Kao, C., Konrad, P., Milner, T., Kim, J., Mahadevan-Jansen, A., & Jansen, E. D. (2007). Biophysical mechanisms of transient optical stimulation of peripheral nerve. *Biophys. J., 93*(7), 2567-2580. doi:10.1529/biophysj.107.104786

World Health Organization. (2018). Addressing the rising prevalence of hearing loss. *Available at: https://apps.who.int/iris/handle/10665/260336 [Accessed 7 September 2022]*.

World Health Organization. (2019). New WHO-ITU standard aims to prevent hearing loss among 1.1 billion young people. *Available at: https://www.who.int/news/item/12-02-2019-new-who-itu-standard-aims-to-prevent-hearing-loss-among-1.1-billion-young-people [Accessed 7 September 2022]*.

World Health Organization. (2021). Deafness and hearing loss. *Available at: https://www.who.int/news-room/fact-sheets/detail/deafness-and-hearing-loss [Accessed 7 September 2022]*.

Yamamoto, K., Yamada, K., Yatagai, S., Ujihara, Y., & Toda, K. (2022). Spatiotemporal Pavlovian head-fixed reversal learning task for mice. *Mol. Brain., 15*(1), 78. doi:10.1186/s13041-022-00952-5

Yeung, J., Griffin, A., Newton, S., Kenna, M., & Licameli, G. R. (2018). Revision cochlear implant surgery in children: Surgical and audiological outcomes. *Laryngoscope, 128*(11), 2619-2624. doi:10.1002/lary.27198

Young, H. K., Tan, X., Xia, N., & Richter, C. P. (2015). Target structures for cochlear infrared neural stimulation. *Neurophotonics, 2*(2), 025002. doi:10.1117/1.NPh.2.2.025002

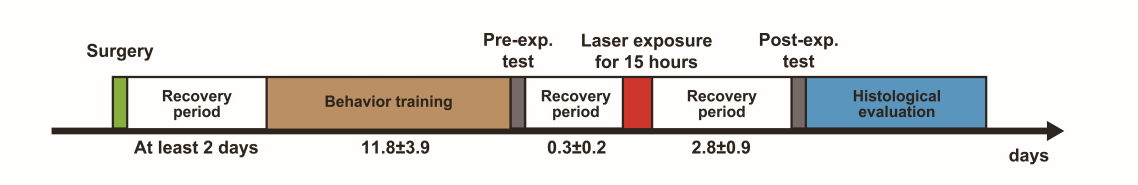

Figure 1. Time course of the experiment. Before head-fixed classical conditioning, surgery was performed to set the head plate and recording electrode on the subjects and to impair hearing sensitivity in the right ear. At least two days after the surgery, the training session was conducted to associate the relationship between the auditory cue and the liquid reward for 11.8 ± 3.9 days (Mean ± SEM, n=18). The pre-exposure test was conducted after the training was completed. Subsequently, continuous laser exposure was presented for 15 h after recovery (0.3 ± 0.2 days). The cochlear response was recorded during the laser exposure. The post-exposure test was carried out 2.8±0.9 (Mean±SEM) days after the laser exposure. Finally, the subjects were euthanized on the same day as the post-exposure test, and histological inspection was performed.

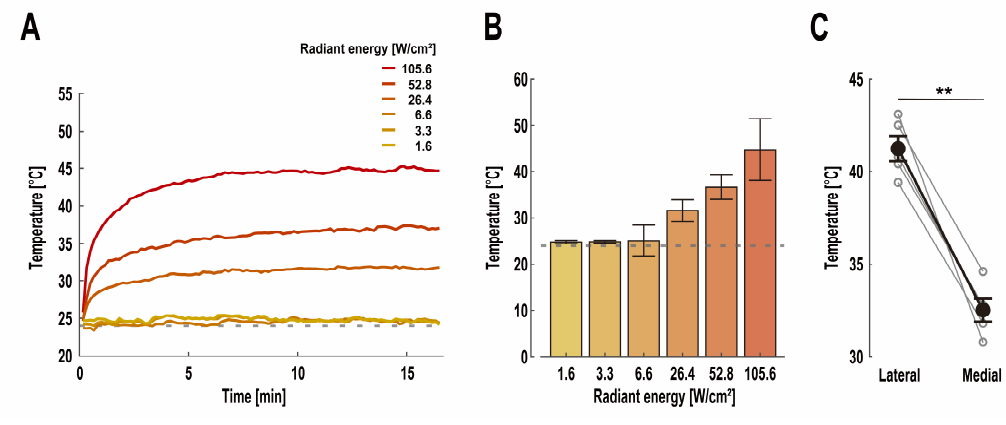

Figure 2. Thermal elevation of the cochlear surface caused by laser irradiation. (A) Time course of the average temperature rise on the irradiation site of the cochlear surface. (B) Surface temperature at 10 min after the laser onset in (A). Error bars indicate the standard deviation (1.6 W/cm^2: n = 3, others: n = 4). (C) Temperature difference between the lateral and medial sides of the cochlear surface following the laser irradiation of 105.6 W/cm^2 (n=5). Glay open circles show the temperature in each cochlea. In (A) and (B), the gray dotted line shows the room temperature (24 °C). Error bars describe the standard error of the mean. **: $P < 0.01$.

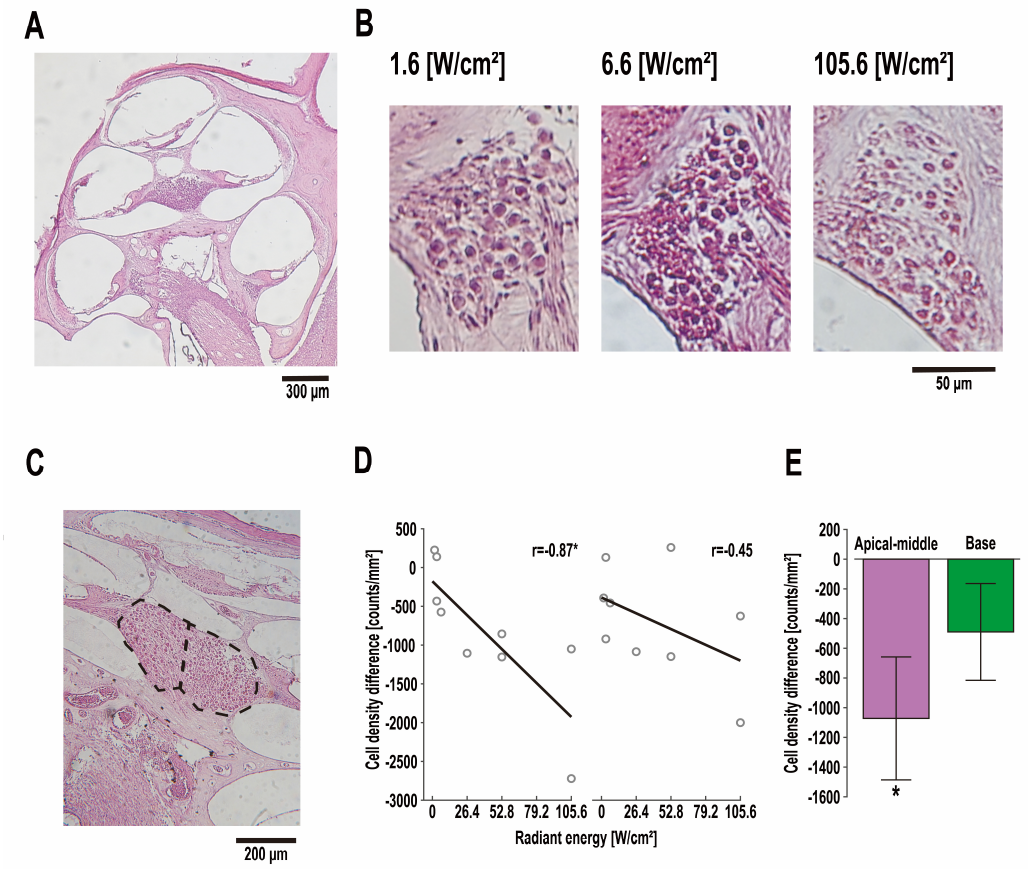

682

683

684 **Figure 3. Laser-induced lesion in spiral ganglion neurons.** (A) Horizontal section of

685 laser irradiated cochlea showing all turns (radiant energy: 6.6 W/cm^2). (B) Density of

686 spiral ganglion neurons in the lateral side of the basal turn after laser exposure of 1.6

687 W/cm^2 (left), 6.6 W/cm^2 (middle), and 105.6 W/cm^2 (right). (C) Lateral (left) and medial

688 (right) sides of the spiral ganglion neuron density in middle turn. The dotted line separates

689 the lateral and medial sides of the spiral ganglion area in the middle turn. (D) Change in

690 the cell density after laser exposure on lateral (left) and medial (right) sides of the cochlea.

691 The cell density difference was defined as the mean spiral ganglion density difference
692 between the laser irradiated (left ear) and the opposite (right ear) cochlea. Gray open
693 circles indicate individual data. Correlation coefficients were calculated using Pearson's
694 correlation analysis. (E) Mean cell density difference between the laser irradiated and
695 opposite cochlea in apical-middle (left) and basal (right) turn on the lateral side. Data
696 from all radiant energy conditions were pooled in the analysis. *: $P < 0.05$.

697

698

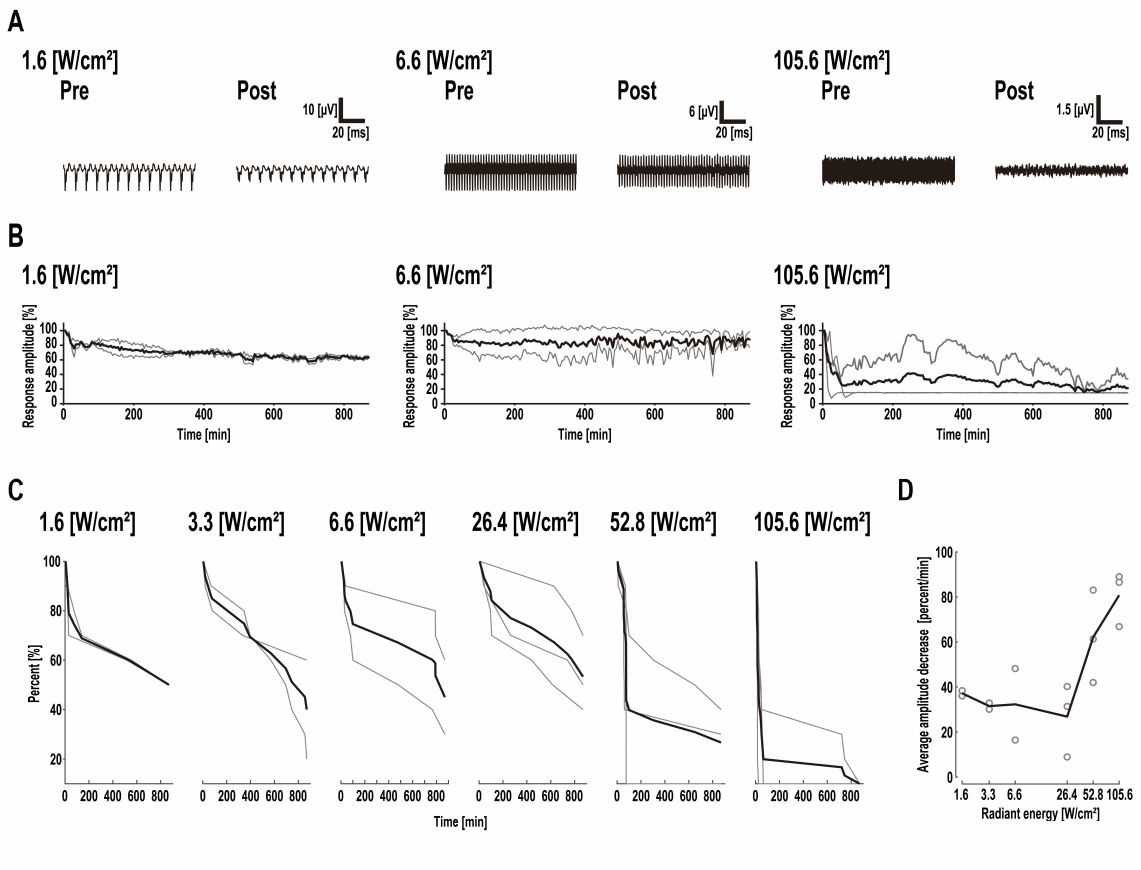

Figure 4. Cochlear function assessment during continuous laser exposure. (A) Cochlear response during continuous pulsed laser irradiation of 1.6 (left), 6.6 (middle), and 105.6 (right) W/cm^2 (i.e., 125, 500, and 8000 pulses/s). (B) Time course of the cochlear response amplitude elicited by the 1.6 (left), 6.6 (middle), and 105.6 (right) W/cm^2 laser stimulation. (C) Relationship between laser irradiation time and percent of the response amplitude. (D) Average amplitude decrease caused by continuous laser irradiation depending on the radiant energy. Gray open circles indicate individual data. Gray lines in (B) and (C) show individual data.

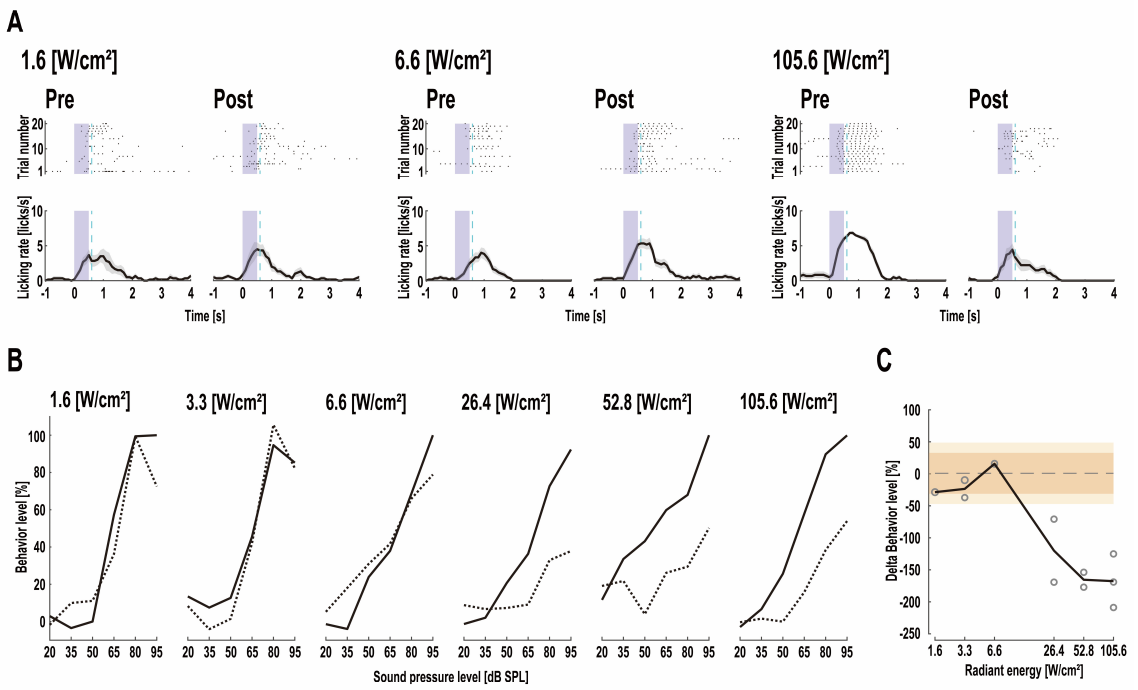

Figure 5. Influence of continuous laser irradiation on the auditory-evoked behavioral response. (A) Auditory-evoked licking behavior pre- and post-laser exposure of 1.6 (left), 6.6 (middle), and 105.6 (right) W/cm^2. Individual trials and mean peri-stimulus time histograms (PSTH) of the licking behavior elicited by auditory stimuli (80 dB SPL) are shown in top and bottom figures, respectively. The blue zones indicate auditory stimulation periods. The light blue dotted lines show the reward timing in the training trials. Black plots in the top figure show licking timing. (B) Behavioral level alternation after continuous laser irradiation. Solid and dotted lines show pre- and post-behavioral levels, respectively. The behavioral level was determined as the ratio of delta

licking rate over the maximum delta licking rate of the pre-laser exposure (1.6 W/cm^2: n=1, 3.3 W/cm^2: n=2, 6.6 W/cm^2: n=2, 26.4 W/cm^2: n=2, 52.8 W/cm^2: n=2, 105.6 W/cm^2: n=3). (C) Change in the delta behavioral level between pre- and post-laser exposure. In the control condition, delta behavioral level was measured by comparing the pre- and post-placing the subjects on the experimental setup for 15 h (n=9). Gray dotted line shows the mean of the delta behavioral level in the control condition, and colored areas indicate two (red) and three (orange) standard deviations. The safety margin was determined as the mean ± three standard deviations (i.e., orange area). Gray open cycles represent delta behavioral response in each subject (n = 18).

Supplemental Figures

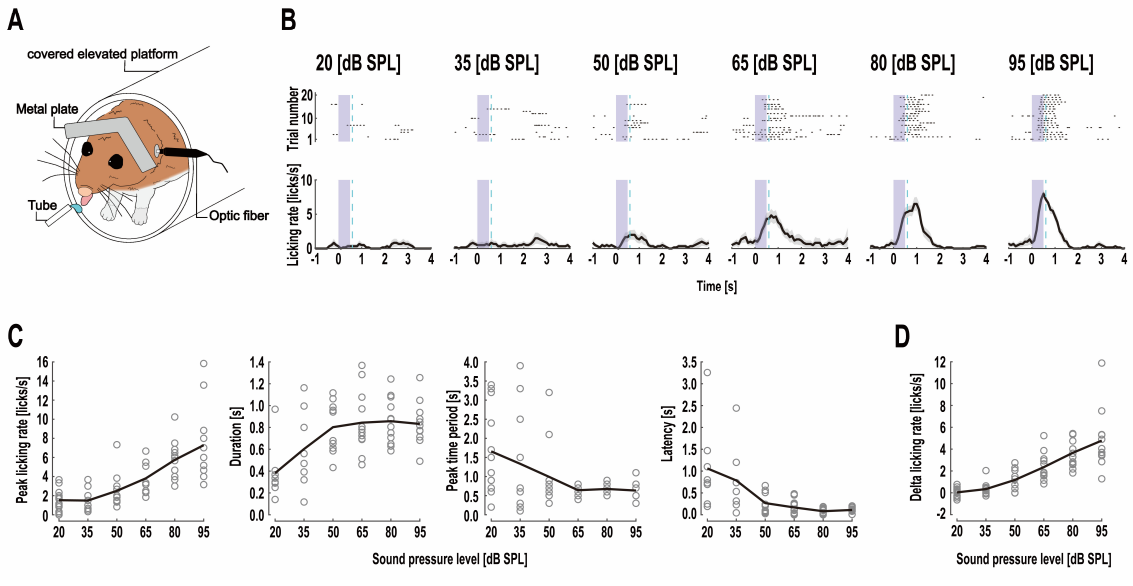

Supplemental Figure 1. Auditory-induced licking behavior in head-fixed Mongolian gerbils and behavioral profile depending on the sound pressure level. (A) Schematic of the head-fixed setup. We investigated the perception of auditory stimuli by using head-fixed classical conditioning. A drop of water was delivered through the tube after presenting white noise, and the timing of licks was recorded using a touch sensor, as in previous studies. (B) Individual trial (top) and mean peri-stimulus time histogram (PSTH) (bottom) of the licking behavior elicited by auditory stimuli with various sound pressure levels. The blue zones indicate auditory stimulation periods. The light blue dotted lines show the reward timing in the training trials. Black plots in the top figure show licking

timing. Increasing the intensity of white noise elicited a systematic change in behavioral responses. (C) Intensity dependence of the peak licking rate, duration, peak time period, and latency. As the sound pressure level increased from 20 to 95 dB SPL, peak licking rate was increased from 1.52 to 7.28 licks/s, duration was increased from 0.38 to 0.83 s, peak period was decreased from 1.66 to 0.63 s, latency was decreased from 1.06 to 0.11 s. (D) Mean auditory-evoked delta licking rate. The delta licking rate was defined as the response amplitude to quantify the response amplitude of licking behavior. The delta licking rate significantly increased from 0.04 to 4.78 licks/s depending on the intensity of the white noise. In (C) and (D), the open grey cycles show the individual data (n=12).

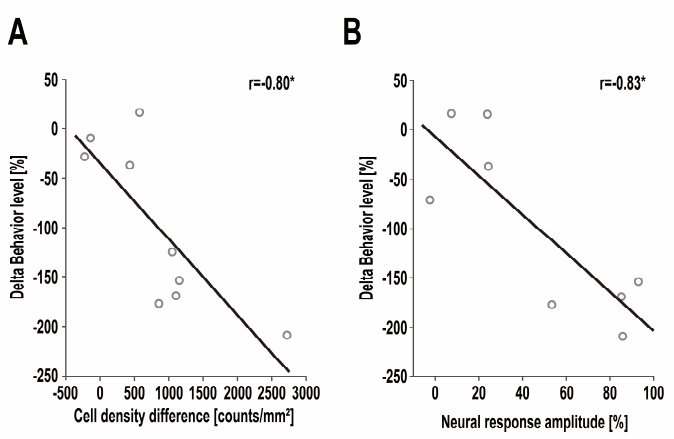

Supplemental Figure 2. Change in the delta behavioral level depending on the decrease in the cell density difference (A) and neural response amplitude (B). Histological and behavioral data (n=9) or electrophysiological and behavioral data (n=8) were obtained from the subjects. The correlation coefficients were calculated using Pearson's correlation analysis. As the spiral ganglion neuron density decreased, the delta behavioral level significantly decreased (r=-0.80, P<0.05, Pearson's correlation analysis). A similar tendency was observed in the relationship between the decrement of the cochlear response and behavioral response; the decreasing amplitude of the cochlear response significantly reduced the behavioral response (r=-0.83, P<0.05, Pearson's correlation analysis). These results suggest that auditory perception is affected by the physiological deterioration of the cochlea. The open circles indicate individual data. *: *P* < 0.05.